Effective Bandwidth for Delay Tolerant Secondary User Traffic in Multi-PU, Multi-SU Dynamic Spectrum Access Networks

Ebrahim Safavi and K.P. Subbalakshmi
Department of Electrical and Computer Engineering, Stevens Institute of Technology
Email: {ssafavi,ksubbala}@stevens.edu

Abstract

In this paper we study two important quality of service (QoS) parameters of dynamic spectrum access (DSA) networks with multiple primary and secondary users. We assume that the SUs are delay tolerant and model the PU and SU activity as Markov chains with ON and OFF states. We derive a closed form expression for the probability distribution of buffer occupancy for secondary networks under steady state conditions and formulate an expression for the effective bandwidth under buffer overflow constraints. Extensive simulations are used to validate our analysis.

Index Terms

Dynamic Spectrum Access, Multi-Primary and Multi-Secondary Users, Effective Bandwidth, Buffer occupancy, Asymptotic Tail Behavior.

I. Introduction

Dynamic Spectrum Access (DSA) networking has received significant attention [1]–[16] due to its potential impact in reducing spectrum wastage. While spectrum utilization in cognitive radio networks (CRN) is a well-researched topic [12]–[19], the limits and capabilities of the CRN under quality of service (QoS) constraint, which is an important problem from a practical perspective, are just beginning to be studied [3]–[7], [20], [21]. In this paper we address two

important QoS parameters of DSA networks: (1) the effective bandwidth and, (2) the tail behavior of the transmission buffer.

Effective bandwidth is defined as the maximum reliable bandwidth that a network can provide under some predefined QoS constraints [22]. It also reflects the efficiency of resource allocation in the network [23]. In this paper, we investigate the effective bandwidth available to secondary users (SUs) subject to some maximum buffer overflow probability. We assume delay tolerant secondary network traffic, where the traffic generated by SUs is buffered for future service when no networks are available (due to primary network activity or otherwise).

The tail behavior of this queue is another important QoS characteristic for such networks. Networks with heavy-tailed distributions show significantly different behavior from that of the light tailed (e.g., exponential) distribution. More specifically, a heavy tailed distribution on the queue length can drastically degrade the network performance, by either reducing the network throughput and stability or introducing infinite moments like mean and variance [24].

Our work proposes an analytically tractable finite-state Markov model to jointly describe the PU and SU network, which leads us to the main contributions of the paper:

1) Closed-form expression for the probability distribution of the buffer occupancy for secondary networks under steady state conditions,
2) Formulation and expression for the effective bandwidth under buffer overflow constraints,
3) Analysis of sufficient conditions for light-tailed buffer occupancy distributions for a general CRN with multiple SUs and multiple PUs.

We model the CRN consisting of an arbitrary number of SUs and PUs as a continuous time Markov model, where network users can switch ON and OFF at any time [4], [6], [12]. Also, when a PU turns ON, the channel associated with that PU (primarily licensed to it) is unavailable for use by any SU. We assume that SUs can dynamically move to another band upon the return of the PU. The buffer behavior for this system is formulated as a stochastic fluid flow model [7], [25]–[33]. This approximation assumes that the system dynamics depend on the aggregate behavior of packets rather than individual packets, and is more applicable to situations where the individual data packet size is a very small fraction of the typical buffer size [32]. The computational complexity of the fluid models is polynomial in the number of system states [25].

A. Related Work

Examples of studies on effective bandwidth for wireless networks can be found in [3], [6], [34]–[36]. Studies on QoS parameters of CRN include [6], [7], [13], [27]. In [7], the distribution moments of the SU queue length in light traffic regime for a contention enabled network are calculated. The expressions for the first moments of queue length and waiting time in a CRN are derived using a priority model for primary and secondary networks in [13]. The main problem with priority level models is that they don't capture some nuances of DSA networks. For instance, *priority models do not allow for the fact that an SU (lower priority user) can still transmit when a PU switches ON, by switching to another unoccupied channel. Our current model is able to address this deficiency.* The effective bandwidth in random channel access networks is studied in [6], where the optimal queue performance for the aggregate system is formulated. Unlike [6] which models the activities of SUs independent of activities of PUs, we take into account the channel availability to reflect the impact of PU activities on QoS parameters.

In [37], the effective capacity for pre-assumed light-tailed distribution of the queue occupancy is analyzed where a *single* channel is shared among PUs and the cognitive user. In contrast to [37], we analytically derive the distribution of the buffer occupancy for the CRN and also analyze the effective bandwidth available to cognitive users that have access to an arbitrary number of channels.

QoS provisioning on the buffer size and delay in voice service is studied in [38], where the admission control in the secondary network with respect to a pre-fixed packet drop probability is analyzed. The system model [38] comprises of a single wireless channel shared among all PUs and SUs.

The effective bandwidth and asymptotic tail behavior of delay distribution for SUs in single-channel DSA networks was analyzed using the law of large numbers in [12]. A large deviation approximation of the queue length distribution as a function of the PU and SU traffic was investigated in [4]. Both [12] and [4] concluded that the delay and buffer occupancy distributions for the network consisting of a single PU are light-tailed if the busy period is light-tailed. The asymptotic analysis of the steady-state queue length distribution of SUs for a single PU channel under heavy-tailed network environment is considered in [5].

Unlike [12] and [4] which derive *approximations* for the *tail* end of the distribution in *single*

PU channel networks, we derive the *exact closed-form expression of the buffer occupancy for a general secondary network comprising multiple channels over the entire range.* We also analyze the asymptotic tail behavior of buffer occupancy distribution of general multi-channel DSA networks and show that *if the busy period distribution for PUs are light-tailed, then the buffer occupancy for multi-SU, multi-PU network is also a light-tailed distribution.*

The effective capacity for the coexisting CRNs in Nakagami wireless fading channels with respect to some delay constraints is addressed in [39]. In [35], the Gaussian throughput for a CRN coexisting with a primary network is investigated, where the impact of the primary network is modeled as an interference channel. The effective capacity for an underlay CRN with a single primary and secondary link subject to the average interference and delay constraints is addressed in [36], which calculates some bounds on the effective capacity of the model.

Effective bandwidth for a general multi-SU multi-PU DSA networks has not yet been fully explored for dynamic spectrum enabled CRNs. This work studies the effective bandwidth performance for such networks under certain QoS provisioning.

The organization of this paper is as follows. In Section II, we consider CRNs with homogeneous wireless channels and provide our mathematical model for the network. We also review the effective bandwidth theory. The asymptotic analysis of the buffer occupancy distribution is provided in Section III. In Section IV, the effective bandwidth for different network realization is formulated. In Section V we provide some numerical examples to validate our analysis and to investigate the queueing performance. We conclude our study in Section VI .

II. System Model

Our system model comprises of an arbitrary number, N_s, of homogeneous SUs that independently switch between active and idle states. The SUs generate data at rate c_s bits per second (bps) during the active periods, whether or not it has access to a channel for transmission. The transmission activities of SUs are modeled as N_s independent identically-distributed (i.i.d.) Poisson processes, where the intervals between consecutive events (active and idle states) are i.i.d. exponential random variables. This model is able to capture the burstiness of the data stream [31].

Since a given channel is essentially unavailable to the CRN upon the return of the PU, channels can also be modeled as ON-OFF processes. We model the PU network, comprising N_p

homogenous PUs as a continuous time Markov chain (CTMC). Each channel can exist in one of two states: free (when the associated PU is OFF) or busy (when the associated PU is ON). Each channel has c_p bps capacity. The channel free/busy time is shown in Fig. 1. The channel is busy for a random time period $T_{\rm b} \propto \exp(\lambda_p)$ and is free for a random time period $T_{\rm f} \propto \exp(\mu_p)$. The summary of system parameters are identified in Table I.

We assume that there exists a spectrum availability database through which the spectrum availability is perfectly known. This assumption is reasonable since as per the President Council of Advisors on Science and Technology's report, there is a shift towards a database approach for deciding spectrum availability (away from the spectrum sensing approach) [40]. When sensing based dynamic spectrum access is the predominant alternative, there can be imperfections in the sensing mechanisms leading to the imperfect knowledge about spectrum bands. We leave this case for future work.

For a fixed access policy π, let $Q^\pi(t)$ denote the queue size of the tagged SU at time t. Then, the buffer content of the SU for the next Δt seconds can be modeled as a Lindley process [41] satisfying the following equation [4]:

$$Q^\pi(t+\Delta t) = (Q^\pi(t) + c_s \Delta t - c^\pi(t+\Delta t))^+,\ Q^\pi(0) = 0 \tag{1}$$

where $c^\pi(\cdot)$ shows the output channel available to the tagged SU at a given time and $(\cdot)^+$ shows the positive portion. At given time t, the aggregate buffer occupancy, $Q^\pi(t)$ is a measure of the performance of the secondary network.

In our study, we are interested in characterizing the queue performance of the first-in first-out (FIFO) channel access policy when there is perfect knowledge about spectrum bands for SUs determined by the spectrum availability database. From now on, we shall omit the π superscript.

A. Effective Bandwidth

The effective bandwidth is the minimum constant service rate required to guarantee a given QoS, θ. For a given stationary service process, $C(t)$, the effective bandwidth of the service process is [22]:

$$\mathcal{C}(\theta) = -\frac{\Psi_C(-\theta)}{\theta}, \quad \forall \theta > 0 \tag{2}$$

where $\Psi_C(\cdot)$ is Gärtner-Ellis limit defined as

$$\Psi_C(\theta) = \lim_{t\to\infty} \frac{1}{t} \log \mathbf{E}[e^{\theta C(t)}], \quad \theta > 0 \tag{3}$$

and, $\mathbf{E}[\cdot]$ stands for the expected value and $\mathcal{C}(\theta)$ is the maximum *constant* arrival rate that can be supported for the QoS parameter θ. Throughout this paper, serving data means assigning one channel to the data stream for transmission.

When the queue is stable and Gärtner-Ellis limit exists, and there is a unique positive solution, θ^*, to the equation:

$$a\theta + \Psi_C(-\theta) = 0, \tag{4}$$

the buffer overflow probability of a given buffer value q is independent of time index[1], t, and has the following form:

$$\Pr(Q > q) = \mathcal{O}(e^{-\theta^*(a)q}), \tag{5}$$

where $\mathcal{O}(\cdot)$ denotes the Big-O asymptotic notation, a is the maximum sustainable arrival rate (the effective bandwidth), and $\theta^*(a)$ is the decay rate of the overflow probability which is the inverse function of the effective bandwidth of the arrival process (i.e. $\mathcal{C}(\theta^*) = a$) [4].

In CRNs, due to the dependence between arrival and service processes through the sensing mechanism, the effective bandwidth is a function of both the arrival and service processes. In the following, we use the buffer overflow probability of the dependent system as the QoS indicator to evaluate the effective bandwidth. The key point is that for the service process modeled by $\theta^*(a)$ at given buffer bound $q \gg 1$, and QoS parameter $\epsilon \ll 1$, the effective bandwidth a should satisfy the approximation $\epsilon \approx e^{-q\theta^*(a)}$.

The objective of this paper is to obtain the maximum sustainable arrival rate $a^*(\epsilon)$ which, by definition, is the effective bandwidth of the system, calculated for a given value of buffer size, q, and ϵ overflow probability:

$$a^*(\epsilon) = \arg \sup_a \{\Pr(Q > q) \leq \epsilon\}. \tag{6}$$

In the following section, we model the arrival and service processes in the CRN. Later, we find the closed-form expression for the probability distribution function (pdf) of the buffer occupancy, to evaluate the effective bandwidth.

[1]So, we can drop the t-dependency index

B. Cognitive Radio Network with Single Primary Channel

Before proceeding with a general network, we consider the simple network consisting of a single SU and a single PU to explain the method. Let $P_{\mathrm{f}}(q,t)$ be the cumulative distribution function (CDF) of the buffer occupancy at given time t when the channel is in the free state, that is:

$$P_{\mathrm{f}}(q,t) = \Pr\left\{Q(t) \leq q, T_{\mathrm{f}}\right\}, \tag{7}$$

where $Q(t)$ denotes the buffer content at time t and T_{f} is period for which the channel is free, as defined earlier. The CDF when the channel is busy, $P_{\mathrm{b}}(q,t)$, also can be defined in the same way. The distribution parameters for active and idle periods for the PU are λ_p and μ_p, respectively. Therefore, the probability that the PU switches from the idle state to the busy state (channel state switches from free to busy) in the next Δt seconds is $\mu_p \Delta t$. The probability that no transition happens is $1-\mu_p\Delta t$. In this case, the amount of depletion of the buffer content is $(c_p - c_s)\Delta t$. Therefore, the buffer occupancy CDF for the next Δt second, $P_{\mathrm{f}}(q, t+\Delta t)$, is:

$$\lambda_p \Delta t P_{\mathrm{b}}(q,t) + (1-\mu_p\Delta t) P_{\mathrm{f}}(q + (c_s - c_p)\Delta t, t) \tag{8}$$

Similar equations can be written for the CDF of buffer occupancy when the PU is in the busy state. However, here due to the lack of access to the channel, the increase in the buffer content is $c_s \Delta t$. Therefore, we have:

$$P_{\mathrm{b}}(q, t+\Delta t) = \mu_p \Delta t P_{\mathrm{f}}(q,t) + (1-\lambda_p\Delta t) P_{\mathrm{b}}(q + c_s\Delta t, t) \tag{9}$$

Solving Eq. (8) and (9) for infinitesimally small Δt value, we have:

$$(c_p - c_s)\frac{\partial P_{\mathrm{f}}}{\partial q} + \frac{\partial P_{\mathrm{f}}}{\partial t} = \lambda_p P_{\mathrm{b}} - \mu_p P_{\mathrm{f}} \tag{10}$$

and

$$-c_s \frac{\partial P_{\mathrm{b}}}{\partial q} + \frac{\partial P_{\mathrm{b}}}{\partial t} = \mu_p P_{\mathrm{f}} - \lambda_p P_{\mathrm{b}} \tag{11}$$

In our analysis, we are interested in steady state behavior, hence the probability distribution has no time variation and we can drop time dependency index. To uniquely determine the solution for the set of first order differential equations in Eq. (10) and (11), the knowledge of boundary condition is necessary. When there is no constraint on the buffer content (i.e. $q = \infty$), the probability of being in the free or busy states is $P_{\mathrm{f}}(\infty) = \frac{\lambda_p}{\lambda_p+\mu_p}$ and $P_{\mathrm{b}}(\infty) = \frac{\mu_p}{\lambda_p+\mu_p}$. In

addition, in the busy state, when no channel is available, the buffer should always be non-empty, i.e. $P_{\rm b}(0) = 0$.

Using the boundary conditions, the solutions for buffer occupancy CDF in free and busy states are the summation of exponentials $P_{\rm f}(q) = \alpha_1 e^{-\theta q} + \alpha_2$ and $P_{\rm f}(q) = \beta_1 e^{-\theta q} + \beta_2$, where:

$$\theta = \frac{\lambda_p}{c_s} - \frac{\mu_p}{c_p - c_s} \tag{12}$$

and $\alpha_1 = \frac{c_s \mu_p}{(c_p - c_s)(\mu_p + \lambda_p)}$ and $\alpha_2 = \frac{\lambda_p}{\lambda_p + \mu_p}$, and also $\beta_1 = -\beta_2 = -\frac{\mu_p}{\mu_p + \lambda_p}$. To have bounded CDF functions, the decay rate, θ, should be positive which results:

$$c_s < c_p \frac{\lambda_p}{\lambda_p + \mu_p} \tag{13}$$

where the LHS term is the input rate and the RHS expression denotes the average output rate. Inequality (13) is also known as the stability condition, which is the long-time average input rate compared to the output rate. Using Bayes' rule, the buffer occupancy CDF, $P(\cdot)$, can be expressed as $P(q) = P_{\rm b}(q) + P_{\rm f}(q)$. Eq. (12) shows that when $c_s \to c_p \frac{\lambda_p}{\lambda_p + \mu_p}$, the buffer occupancy CDF decays very slowly with respect to the buffer size.

Using the buffer occupancy CDFs in free and busy states, the buffer overflow probability is $\Pr(Q > q) = 1 - P(q)$. Hence, we have:

$$\Pr(Q > q) = \frac{\mu_p}{\mu_p + \lambda_p} \frac{c_p}{c_p - c_s} e^{-\theta q} \tag{14}$$

Following Eq. (6), for the buffer size q and the overflow probability ϵ, the effective bandwidth, a^* can be calculated as the solution to the nonlinear equation $\Pr(Q > q) = \epsilon$. Finding a closed-form expression for this equation is very difficult, however, we can study some special cases. For example, for small value of buffer size, q, the effective bandwidth is significantly smaller than channel PU's channel capacity, $a^* \ll c_p$. Therefore, the effective bandwidth is given by:

$$a^*_{a^* \ll c_p} \approx \frac{\lambda_p c_p q}{\mu_p q - c_p \log \epsilon'} \tag{15}$$

where $\epsilon' = \epsilon(1 + \lambda_p/\mu_p)$. Therefore, the maximum rate that the SU can use to transmit its data with the buffer size q at the maximum buffer overflow probability ϵ is when $c_s = a^*$. However, for a large buffer size, $q \gg 1$, the effective bandwidth is the maximum possible transmit rate for the stable system:

$$\lim_{q \to \infty} a^* = c_p \frac{\lambda_p}{\lambda_p + \mu_p} \tag{16}$$

The analysis carried out in the case of single PU can be generalized to the case $N_p > 1$. In what follows, we extend our analysis to the general case when $N_s, N_p \geq 1$ and SUs can also switch between active and idle states.

C. General Cognitive Radio Network

We again model the system as a CTMC. Let the number of SUs in the active state, at time t, be i and the number of idle channels be j; the network system state is represented by the two-tuple $s = (i, j)$. The total number of possible states is $(N_s+1)\times(N_p+1)$. The corresponding distribution parameters for active and idle periods for SUs are λ_s and μ_s, respectively. Therefore, the average time for the active and idle periods for an SU are λ_s^{-1} and μ_s^{-1}, respectively.

When the PU turns active, the corresponding channel (licensed to the PU) is unavailable for use by any SU. However, an SU in that band can look for and occupy any vacant channel upon the return of the PU to its current channel. If any SU generates data when there is no available channel, the data traffic goes into a buffer associated with that SU (see Fig. 2).

Each SU buffers its data stream until it gains access to the transmission channel in accordance with the FIFO rule i.e., each SU should wait until all prior channel requests are processed. Therefore, we can model the entire system of buffers as a single virtual aggregate buffer, $Q(\cdot)$, where the content of the aggregate buffer is the summation over the content of all individual SU buffers (see Fig. 2). The aggregate buffer drift rate at any state, $c_{i,j}$ depends on the number of free channels and active SUs. The available channel capacity at any state and time is:

$$c_{i,j} = jc_p - ic_s \tag{17}$$

Let $P_{i,j}(q,t)$, $i \in [0, N_s]$, $j \in [0, N_p]$ and $t, q \geq 0$, be the CDF of the aggregate buffer occupancy probability that at the time t, i SUs are in active and j PUs are in idle states, and the total content of all SU buffers does not exceed q i.e.

$$P_{i,j}(q,t) = \Pr\{Q(t) < q \text{ and } s = (i,j)\} \tag{18}$$

As long as the buffer is not empty, the aggregate buffer is depleted at the instantaneous rate $c_{i,j}$. Once all buffers are empty, they stay in the empty state as long as the combined data rate of all SUs is less than the available channel capacity, that is $ic_s < jc_p$. The CDF of aggregate buffer

occupancy, $P(\cdot)$, can be expressed as a summation of $P_{i,j}$'s:

$$P(q,t) = \sum_{i \leq N_s, j \leq N_p} P_{i,j}(q,t) \tag{19}$$

We assume an infinite buffer for all SUs. For such a system, the stability condition is satisfied if the long-time average input traffic rate, D_{in}, for the entire secondary network is less than the long-time average throughput rate, D_{out}. It is easy to show that the average network input traffic rate is $D_{\text{in}} = N_s c_s \frac{\mu_s}{\lambda_s + \mu_s}$, and the average throughput is $D_{\text{out}} = N_p c_p \frac{\lambda_p}{\lambda_p + \mu_p}$. We define the stability ratio parameter, $\rho = \frac{D_{\text{in}}}{D_{\text{out}}}$. The system is said to be stable if the system stability ratio parameter, ρ is less than unity.

The assumption of the CTMC system model allows us to characterize the aggregate buffer occupancy probability distribution using Kolmogorov's backward equations. Since the periods of idle and active states for the SUs are exponentially distributed, the probability that for the next Δt time slot, an SU turns ON or OFF can be written as $(N_s - i)\mu_s \Delta t + \mathcal{O}(\Delta t^2)$ and $i\lambda_s \Delta t + \mathcal{O}(\Delta t^2)$, respectively, where $\mathcal{O}(\cdot)$ is the Big-O asymptotic notation. Similarly, for the PUs, these probabilities are $j\mu_p \Delta t + \mathcal{O}(\Delta t^2)$ and $(N_p - j)\lambda_p \Delta t + \mathcal{O}(\Delta t^2)$, respectively. The probability of any compound event is $\mathcal{O}(\Delta t^2)$. The probability that there is no change in the states of the PU or SU is given by $1 - ((N_s - i)\mu_s + i\lambda_s + j\mu_p + (N_p - j)\lambda_p)\Delta t + \mathcal{O}(\Delta t^2)$. Assuming Δt is infinitesimally small, we can ignore higher order terms, $\mathcal{O}(\Delta t^2)$, and use CTMC to derive the following partial differential equations.

$$\begin{aligned} \frac{\partial P_{i,j}}{\partial t} - c_{i,j} \frac{\partial P_{i,j}}{\partial q} = (N - i + 1)\mu_s P_{i-1,j} + \\ (i+1)\lambda_s P_{i+1,j} + (j+1)\mu_p P_{i,j+1} + (M - j + 1)\lambda_p P_{i,j-1} \\ -((N-i)\mu_s + i\lambda_s) + j\mu_p + (M-j)\lambda_p) P_{i,j} \end{aligned} \tag{20}$$

where $P_{i,j} = P_{i,j}(q,t)$. At steady state, the probability distribution does not change with respect to time ($\partial P_{i,j}/\partial t \to 0$). Therefore, the first LHS term in Eq. (20) will vanish at steady state, and hereafter, we can drop the time index t, for probability functions. The state transition diagram is shown in Fig. 3. Using matrix notation, we can reformulate Eq. (20) as:

$$\mathbf{A} \frac{d}{dq} \mathbf{P}(q) = \mathbf{B}\mathbf{P}(q) \tag{21}$$

where $\mathbf{P}(\cdot) = [P_{0,0}(\cdot), \cdots, P_{i,j}(\cdot), \cdots, P_{N_s,N_p}(\cdot)]'$, and its dimension is the same as the state-space dimension. Let z be an eigenvalue of $\mathbf{A}^{-1}\mathbf{B}$ and $\boldsymbol{\phi}$ be the associated right eigenvector. That is,

$$z\mathbf{A}\boldsymbol{\phi} = \mathbf{B}\boldsymbol{\phi} \tag{22}$$

Since the primary and the secondary network are independent of each other, $\boldsymbol{\phi}$, the system eigenvector, has Kronecker decomposition of the form $\boldsymbol{\phi}_1 \otimes \boldsymbol{\phi}_2$, where $\otimes$ denotes the Kronecker-product, and $\boldsymbol{\phi}_1$ and $\boldsymbol{\phi}_2$ are eigenvectors of the corresponding independent secondary and primary networks and can be explicitly found using generating polynomials [26].

The bounded solution of the stable system characterized by the first order ordinary differential equation in Eq. (21) can be expressed as:

$$\mathbf{P}(q) = a_0\boldsymbol{\phi}_0 + \sum_{z_l<0} a_l e^{z_l q}\boldsymbol{\phi}_l \tag{23}$$

in which z_l's and $\boldsymbol{\phi}_l$'s are eigenvalues and corresponding eigenvectors of matrix $\mathbf{A}^{-1}\mathbf{B}$. The corresponding coefficient is denoted by a_l.

To uniquely determine the solution of Eq. (21), initial conditions should be specified. If $c_{i,j} \geq 0$ then the depletion rate in aggregate buffer content is positive and therefore, at steady state, the buffer should be empty. In other words, the conditional probability of empty buffer content, given $s = (i, j)$ is $\Pr\{q = 0|s = (i, j)\} = 1$. Therefore, the stationary probability is:

$$P_{i,j}(0) = \pi_i^{\mathrm{su}}\pi_j^{\mathrm{pu}}, \quad c_{i,j} \geq 0 \tag{24}$$

where π_i^{su} is the probability i out of N_s SUs are simultaneously in the active state and π_j^{pu} is the probability that j out of N_p channels are free and can be calculated as:

$$\pi_i^{\mathrm{su}} = \binom{N_s}{i} \frac{\lambda_s^i \mu_s^{N_s-i}}{(\lambda_s+\mu_s)^{N_s}}, \ \pi_j^{\mathrm{pu}} = \binom{N_p}{j} \frac{\mu_p^j \lambda_p^{N_p-j}}{(\lambda_p+\mu_p)^{N_p}} \tag{25}$$

where $\binom{N_s}{i}$ is the total number of i-combinations of N_s objects. On the other hand, if the data rate of the active SUs exceeds the available channel capacity, then under steady state, the buffer content increases and the buffer cannot stay empty. Hence,

$$P_{i,j}(0) = 0, \quad c_{i,j} < 0 \tag{26}$$

The other boundary condition that can be used to determine the solution to Eq. (21) is infinitely large buffer size ($q = \infty$) where, there is no constraint on the buffer content. In this case, the

only non-zero term in Eq. (23) is $\mathbf{P}(\infty) = a_0\boldsymbol{\phi}_0$. For this asymptotic case, $P_{i,j}(\infty)$'s can easily be determined as

$$P_{i,j}(\infty) = \pi_i^{\mathrm{su}}\pi_j^{\mathrm{pu}} \tag{27}$$

Therefore, the total number of unknown equals the number of equations in Eq. (24) and (26), which will enable us to uniquely determine coefficients, a_l's.

Solving Eq. (23), the aggregate buffer occupancy CDF can be found from Eq. (19) and expressed as:

$$P(q) = 1 - \sum_l a_l^{'} e^{z_l q} \tag{28}$$

where $a_l^{'} = -a_l(\mathbf{1} \cdot \boldsymbol{\phi}_l)$, $\mathbf{1}$ denotes the unit vector and $\cdot$ is the inner product operator.

Result 2.1: The aggregate buffer overflow probability is a weighted summation of exponentials for different systems and can be expressed as:

$$\Pr\{Q > q\} = \sum_l a_l^{'} e^{z_l q} \tag{29}$$

Eq. (29) shows that the dominant decay rates, θ^*, can be determined using the system eigenvalues as:

$$\theta^* = -\max_l\{z_l : z_l < 0\} \tag{30}$$

Formulation in Eq. (29) is one of the main contributions of this paper and gives the closed-form expression for the pdf of the secondary network buffer occupancy.

III. Asymptotic analysis of buffer occupancy distribution

In this section, we provide some insight into the asymptotic behavior of the secondary network buffer occupancy and analyze the tail of distribution.

Result 3.1: The buffer occupancy distribution is light-tailed[2] if *the channel busy period distribution is light-tailed.*

[2]A random variable, X, is light-tailed if there is some $\theta > 0$ such that

$$\lim_{x\to\infty} e^{\theta x}\Pr\{X > x\} = 0$$

and if there is no such θ, it is called heavy-tailed random variable.

This can be seen by using the following argument. For the secondary network, we consider the worst case scenario when all SUs are always active by letting $\lambda_s \to 0$. The network buffer overflow probability for any other type of SU activity is smaller for any buffer content value, q.

For a system with the same busy state distribution, the probability that the channel is free for a longer time, is greater for the system with a heavy tailed distribution ($T_{\rm f}^{\rm HT}$) for the free periods compared to a system with a light tailed distribution ($T_{\rm f}^{\rm LT}$) for the free periods. Therefore, the system with $T_{\rm f}^{\rm HT}$ can transmit more often and has less content in the buffer compared to the system with $T_{\rm f}^{\rm LT}$. That is, when the means are the same:

$$\Pr\{Q > q, T_{\rm f}^{\rm HT}\} \leq \Pr\{Q > q, T_{\rm f}^{\rm LT}\} \tag{31}$$

Based on the definition, for any light-tailed free period distribution, $T_{\rm f}^{\rm LT}$, we have:

$$\Pr\{T_{\rm f}^{\rm LT} > t\} \leq e^{-\theta_{\rm f} t}, \tag{32}$$

for some positive $\theta_{\rm f}$. For any light-tailed busy period distribution, we can also find an exponential distribution which satisfies:

$$\Pr\{T_{\rm b}^{\rm LT} > t\} \leq e^{-\theta_{\rm b} t}, \tag{33}$$

for some $\theta_{\rm b} > 0$. Therefore, from Eq. (31), (32) and (33), for any queue system with light-tailed busy period distribution and a given free period distribution, there is a queue system with exponentially distributed busy and free periods such that the former queue system outperforms the latter system. Then, we have:

$$\Pr\{Q > q, T_{\rm b}^{\rm LT}\} \leq \Pr\left\{Q > q, T_{\rm b} \propto \exp(\theta_{\rm b}), T_{\rm f} \propto \exp(\theta_{\rm f})\right\} \tag{34}$$

We already showed in Sec. II-C that for any system with free and busy periods distributed exponentially, the network buffer overflow probability is a summation of exponentials which is a light-tailed distribution. Substituting Eq. (29) in Eq. (34), we have the following inequality:

$$\lim_{q\to\infty} e^{\theta q} \Pr\{Q > q, T_{\rm b}^{\rm LT}\} \leq \lim_{q\to\infty} e^{\theta q} \sum_{l} a_l' e^{z_l q} \tag{35}$$

The RHS expression in Eq. (35) is zero for any $\theta < \theta^*$ (where θ^* is given in Eq. (30)), which implies that *the buffer occupancy has a light-tailed distribution as long as the channel busy state is light-tailed distributed*.

IV. Effective Bandwidth

In general, finding closed-form expression for the effective bandwidth in Eq. (6) is difficult and the overflow probability in Eq. (29) should be numerically evaluated. However, in some special cases good approximations can be made.

A. Effective Bandwidth for Single Channel and Multiple SUs

In the following, we consider the single channel case when the channel is always available ($\mu_p \to 0$). The dominant decay power in this case can be calculated analytically and is:

$$\theta^*_{N_s} = \frac{N_s(N_s c_s \mu_s - c_p(\lambda_s + \mu_s))}{c_p(N_s c_s - c_p)} \tag{36}$$

This can be seen from the following argument. Any eigenvalue z and eigenvector $\boldsymbol{\phi} = (\phi_1, \cdots, \phi_{N_s})$ for the system described in Sec. II should satisfy the following equation [25]:

$$z(ic_s - c_p)\phi_i = \mu_s(N_s + 1 - i)\phi_{i-1} - ((N-i)\mu_s + i\lambda_s)\phi_i \tag{37}$$

$$+(i+1)\lambda_s\phi_{i+1}$$

Then the eigenvector generating power series can be defined as $\phi(x) = \sum_i \phi_i x^i$. Therefore, Eq. (37) can be written in differential form as:

$$\phi(x)(zc_p - N_s\mu_s + N\mu_s x) = \phi^{'}(x)(\mu_s x^2 + (zc_s + \lambda_s - \mu_s)x - \lambda_s) \tag{38}$$

By factorization, the solution to the differential Eq. (38) can be expressed as:

$$\phi(x) = (x - x_1)^k (x - x_2)^{N_s - k} \tag{39}$$

where $k \leq N_s$ is an integer, and

$$x_{1,2} = \frac{-(c_s z + \lambda_s - \mu_s) \pm \sqrt{(c_s z + \lambda_s - \mu_s)^2 + 4\mu_s\lambda_s}}{2\mu_s}. \tag{40}$$

The dominant decay power is the solution to:

$$zc_p - N_s\mu_s + N_s\mu_s x_1 = 0 \tag{41}$$

which results in the following equation:

$$z(4c_p^2 - 4N_s c_p c_s) + (4N_s^2 c_s\mu_s - 4N_s c_p\lambda_s - 4N_s c_p\mu_s) = 0 \tag{42}$$

The solution to the Eq. (42) gives the smallest eigenvalue. From this, the dominant decay power can be found as:

$$z = \frac{N_s(N_s c_s \mu_s - c_p(\lambda_s + \mu_s))}{c_p(N_s c_s - c_p)} \tag{43}$$

The probability distribution in Eq. (29) can be reformulated as:

$$\Pr\{Q > q\} = a_{\theta^*} e^{-\theta^* q} + \sum_{z_l \neq -\theta^*} a_l^{'} e^{z_l q} \tag{44}$$

where a_{θ^*} is the coefficient corresponding to the dominant decay rate. To have a closed-form expression for the effective bandwidth, we can approximate this coefficient as $a_{\theta^*} \approx 1$ [42]. When $q \gg 1$, we can also ignore the RHS summation in Eq. (44). Using Eq. (5), for the overflow probability ϵ and buffer size q, the effective bandwidth can be approximated as:

$$a^*_{N_s}(\epsilon) \approx \frac{N_s c_p(\mu_s + \lambda_s) - c_p^2 \log \epsilon / q}{N_s(N_s \mu_s - c_p \log \epsilon / q)} \tag{45}$$

Eq. (45) shows that the effective bandwidth when $q \to \infty$ is:

$$a^*_{N_s} \to c_p \frac{\mu_s + \lambda_s}{N_s \mu_s} \tag{46}$$

which is the maximum data generation rate for the stable system that happens when the stability ratio is unity, $\rho = 1$.

B. Effective Bandwidth for Single SU and Multiple Channel

This case is the dual of the problem considered in Sec. IV-A. When there are N_p PU channels and SU is always active ($\lambda_s \to 0$), the dominant decay power can be found using the same approach as Sec. IV-A. Then, the dominant decay rate is:

$$\theta^*_{N_p} = \frac{N_p(N_p c_p \lambda_p - c_s(\lambda_p + \mu_p))}{c_s(N_p c_p - c_s)} \tag{47}$$

This can be seen from the following argument. Using the same method as Sec. IV-A, the generating power series can be written in the form of Eq. 39, where

$$x_{1,2} = \frac{(c_p z + \lambda_s - \mu_s) \mp \sqrt{(c_p z + \lambda_p - \mu_p)^2 + 4\mu_p \lambda_p}}{2\lambda_s} \tag{48}$$

In this case, the dominant decay power is the solution to:

$$z c_s - N_p \lambda_p + N_p \lambda_p x_1 = 0 \tag{49}$$

By substitution x_1, the dominant decay power can be found as:

$$z = \frac{N_p(N_p c_p \lambda_p - c_s(\lambda_p + \mu_p))}{c_s(N_p c_p - c_s)} \tag{50}$$

For the specific case $N_p = 1$, the decay rate can be simplified to $\theta^*_{N_p=1} = \frac{\lambda_p}{c_s} - \frac{\mu_p}{c_p - c_s}$, which was also calculated in Eq. (12).

Using the Eq. (44), the effective bandwidth can be approximated as:

$$a^*_{N_p}(\epsilon) \approx \frac{N_p}{2}(c_p + (\lambda_p + \mu_p)q/\log\epsilon) \tag{51}$$
$$+\frac{N_p}{2}\sqrt{(c_p + (\lambda_p + \mu_p)q/\log\epsilon)^2 - 4c_p\lambda_p q/\log\epsilon)}$$

It can be easily verified that for large buffer size ($q \to \infty$) the effective bandwidth will be:

$$a^*_{N_p} \to N_p c_p \frac{\lambda_p}{\lambda_p + \mu_P} \tag{52}$$

Note that the asymptotic effective bandwidth for the network with single SU and single PU with the channel capacity $c_p^{'} = N_p c_p$ is equal to Eq. (52); however, the decay rate is N_p times slower and using Eq. (47), it can be expressed as

$$\theta^{*}_{N_p}{}' = \frac{N_p c_p \lambda_p - c_s(\lambda_p + \mu_p)}{c_s(N_p c_p - c_s)} = \frac{1}{N_p}\theta^*_{N_p} \tag{53}$$

This is also the case for the decay rate of a network comprising a single PU and a single SU with a generation rate $c_s^{'} = N_s c_s$, say $\theta^{*}_{N_s}{}'$ as we have $\theta^{*}_{N_s}{}' = \frac{1}{N_s}\theta^*_{N_s}$.

C. General Case $N_s, N_p \geq 1$

For the general case, finding a closed-form expression for the effective bandwidth is very difficult. However, the dominant decay factor can still be calculated as a root of the following equation [26].

$$N_s\sqrt{P_s(\theta)} + N_p\sqrt{P_p(\theta)} - N_p(c_p\theta + \mu_p + \lambda_p) \tag{54}$$
$$-N_s(-c_s\theta + \mu_s + \lambda_s) = 0$$

where $P_p(\theta) = (c_p\theta + \mu_p - \lambda_p)^2 + 4\mu_p\lambda_p$ and also $P_s(\theta) = (c_s\theta - \mu_s + \lambda_s)^2 + 4\mu_s\lambda_s$. The root of Eq. (54) gives the dominant decay factor, θ^*. After finding θ^*, we use the same approximation as Section IV-A and IV-B. Therefore, Eq. (44) and (54) implicitly express the relationship between the effective bandwidth and the overflow probability, which must be evaluated numerically. For

the special case of large buffer size ($q \to \infty$), the maximum sustainable rate happens when $\rho = 1$. Then the effective bandwidth is:

$$\lim_{q\to\infty} a^* = \frac{N_p c_p \lambda_p}{N_s \mu_s} \frac{\lambda_s + \mu_s}{\lambda_p + \mu_p} \tag{55}$$

V. Numerical Results

In this section, we conduct numerical simulations to illustrate our theoretical results. The parameters of system model used in plotting each figure are identified in Table II.

First, we show the validity of our analysis based on the effective bandwidth theory. In Fig. 4, the activity of 5 SUs and 3 PUs are assumed to be Poisson distributed. The buffer overflow probability, $\Pr\{Q > q\}$ is then obtained by taking the average over 5 simulation runs, where each simulation consists of 1 million time samples with sampling period $\delta = 0.001$ sec. The buffer overflow probabilities for both examples are plotted in Fig. 4. As it can be seen, our analytic results precisely match the simulation results.

Fig. 5a shows the buffer overflow probability distribution of single SU single PU network which is analyzed in Sec. II-B with a fixed packet generation rate ($\rho = 0.7$). Fig. 5a plots the dominant decaying rate, θ^* as a function of buffer size. It also demonstrates that $\log \Pr(Q > q)/q$ converges to θ^* as the buffer size increases. It can be seen that the approximation of the asymptotic decay in Eq. (47) is true even for moderate buffer sizes. For comparison, the simulation results are also provided.

The plot in Fig. 5b shows the effective bandwidth, $a^*(\epsilon)$, versus the QoS exponent, $-\frac{\log \epsilon}{q}$. We fix the overflow probability at $\epsilon = 10^{-3}$ for different buffer sizes, where the numerical evaluation of the theoretical result in Eq. (14) for a given ϵ and buffer size is plotted in solid lines. In [4], the system of a single (always ON) SU with two-state channels is modeled as Markov chain with transition probabilities, $p_{11} = \Pr[\text{free} \to \text{free}]$ and $p_{10} = \Pr[\text{free} \to \text{busy}]$. For the sake of comparison, we study the special case of $p_{11} = p_{01} = \frac{\lambda_p}{\mu_p + \lambda_p}$ and $\lambda_s \to \infty$ to compare our results with the result in [4]. In Fig. 5b, transition probabilities for the Markov chain are $p_{11} = 0.65$ and $p_{10} = 0.35$. In [4], using the approximation $\Pr(Q > q) \approx e^{-\theta^* q}$, the asymptotic effective bandwidth has been provided. From Fig. 5b, it can be seen that the approximation provided in [4] follows the analytical results however, the approximation error increases as the QoS exponent increases.

The dominant decay rate for the network consisting of a single SU with different simulation setups are shown in Fig 6. Fig. 6a shows the dominant decay rate for the system of two PUs with active and idle rates $\lambda_p = 0.4$ and $\mu_p = 0.6$, respectively. To compare results with the study in [4], we set $\lambda_s \to \infty$ (always active SU) and set the transition probabilities $p_{11} = 0.4$ and $p_{01} = 0.6$. The analytical and asymptotic results derived in Eq. (29) and (47) are shown in solid and dash-dot lines, respectively. The lower and upper bounds on the decay rate derived in [4] are also plotted. Fig. 6b shows the decay rate for the network with transition probabilities $p_{11} = 0.8$ and $p_{01} = 0.2$. Fig. 6 verifies our results and shows that our analytical formulations perfectly fit the upper and lower bounds derived in [4].

The effective bandwidth for single channel and also single SU networks are shown in Fig. 7. In Fig. 7a, the effective bandwidth available to each SU for the system of always available single channel with three SUs is plotted. As it can be seen from Fig. 7a, the available effective bandwidth for the zero-size buffer is $a^*_{q=0} = 0.43$ which is the ratio of the channel capacity to the number of SUs, c_p/N_s. However, in Fig. 7b, for the system of multiple PUs where channels alternate between free and busy states, the zero-size buffer effective bandwidth is zero, implying that to have a constant data rate, a non-zero buffer is necessary. Fig. 7b shows the effective bandwidth for the network of a single SU with five PUs. Fig. 7 also shows that effective bandwidth formulations in Eq. (36) and (51) are very good approximations, having less than 1% error for large buffer sizes.

The effective bandwidth for a general network consisting of multiple SUs and multiple PUs (5 SUs and 3 PUs) is shown in Fig. 8. Fig. 8 also depicts the impact of increasing the QoS parameter ϵ on the effective bandwidth for $\epsilon = 10^{-i}, i = \{1, 2, 3, 4\}$.

VI. Conclusion and Future Work

We analyzed the effective bandwidth for a general CRN consisting of multiple PUs and multiple SUs. We defined a stochastic fluid flow model for the SU buffer occupancy and a CTMC to capture the dynamic nature of the PU and SU activities. We obtained the first ever closed-form expression for the effective bandwidth for general DSA networks. We also provided the asymptotic tail distribution analysis for this type of network, where we showed the buffer occupancy is a light-tailed distribution if the busy period for channels are light-tail distributed. Finally, we evaluated our formulations through extensive simulations.

ACKNOWLEDGMENTS

This work was supported in part by NSF Grant No. 1212357.

REFERENCES

[1] E. Hossain, D. Niyato, and Z. Han, *Dynamic Spectrum Access and Management in Cognitive Radio Networks*. Cambridge University Press, 2009.

[2] E. Biglieri, A. J. Goldsmith, L. J. Greenstein, N. Mandayam, and H. V. Poor, *Principles of Cognitive Radio*. Cambridge University Press, 2012.

[3] Q. Wang, D. Wu, and P. Fan, "Effective capacity of a correlated nakagami-m fading channel," *Wireless Communications and Mobile Computing*, vol. 12, no. 14, pp. 1225–1238, 2012.

[4] A. Laourine, S. Chen, and L. Tong, "Queuing analysis in multichannel cognitive spectrum access: A large deviation approach," in *IEEE Conference on Computer Communications Workshops, INFOCOM*, 2010, pp. 1–9.

[5] P. Wang and I. Akyildiz, "Asymptotic queuing analysis for dynamic spectrum access networks in the presence of heavy tails," *IEEE Journal onSelected Areas in Communications*, vol. 31, no. 3, pp. 514–522, March 2013.

[6] G. Hwang and S. Roy, "Design and analysis of optimal random access policies in cognitive radio networks," *IEEE Transactions on Communications*, vol. 60, no. 1, pp. 121–131, January 2012.

[7] S. Wang, J. Zhang, and L. Tong, "A characterization of delay performance of cognitive medium access," *IEEE Transactions on Wireless Communications*, vol. 11, no. 2, pp. 800–809, 2012.

[8] B. Manoj, R. Rao, and M. Zorzi, "Cognet: a cognitive complete knowledge network system," *Wireless Communications, IEEE*, vol. 15, no. 6, pp. 81–88, December 2008.

[9] S. Haykin, "Cognitive radio: brain-empowered wireless communications," *Selected Areas in Communications, IEEE Journal on*, vol. 23, no. 2, pp. 201–220, Feb 2005.

[10] A. Sampath, L. Yang, L. Cao, H. Zheng, and B. Y. Zhao, "High throughput spectrum-aware routing for cognitive radio networks," in *Proc. of International Conference on Cognitive Radio Oriented Wireless Networks and Communications (CROWNCOM)*, 2007.

[11] A. MacKenzie, J. Reed, P. Athanas, C. Bostian, R. Buehrer, L. DaSilva, S. Ellingson, Y. Hou, M. Hsiao, J.-M. Park, C. Patterson, S. Raman, and C. da Silva, "Cognitive radio and networking research at virginia tech," *Proceedings of the IEEE*, vol. 97, no. 4, pp. 660–688, April 2009.

[12] P. Wang and I. Akyildiz, "Can dynamic spectrum access induce heavy tailed delay?" in *IEEE Symposium on New Frontiers in Dynamic Spectrum Access Networks, DySPAN*, 2011, pp. 197–207.

[13] I. Suliman and J. Lehtomaki, "Queueing analysis of opportunistic access in cognitive radios," in *Second International Workshop on Cognitive Radio and Advanced Spectrum Management, CogART*, 2009, pp. 153–157.

[14] M. Rashid, M. Hossain, E. Hossain, and V. Bhargava, "Opportunistic spectrum scheduling for multiuser cognitive radio: a queueing analysis," *IEEE Transactions on Wireless Communications*, vol. 8, no. 10, pp. 5259–5269, 2009.

[15] S. Safavi and K. P. Subbalakshmi, "Optimal joint power allocation and phase control for DS-CDMA cognitive radio networks," in *IEEE Global Telecommunications Conference (GLOBECOM 2011)*, Dec 2011, pp. 1–5.

[16] S. Wang, J. Zhang, and L. Tong, "Delay analysis for cognitive radio networks with random access: A fluid queue view," in *IEEE Conference on Computer Communications, INFOCOM*, 2010, pp. 1–9.

[17] L. Gao, X. Wang, Y. Xu, and Q. Zhang, "Spectrum trading in cognitive radio networks: A contract-theoretic modeling approach," *Selected Areas in Communications, IEEE Journal on*, vol. 29, no. 4, pp. 843–855, April 2011.

[18] A. Azarfar, C.-H. Liu, J.-F. Frigon, B. Sanso, and D. Cabric, "Cooperative spectrum sensing scheduling optimization in multi-channel dynamic spectrum access networks," in *Global Communications Conference (GLOBECOM), 2014 IEEE*, Dec 2014, pp. 810–815.

[19] W. Zhang and R. M. K. Letaief, "Cooperative spectrum sensing optimization in cognitive radio networks," in *Communications, 2008. ICC '08. IEEE International Conference on*, May 2008, pp. 3411–3415.

[20] F. Kocak, H. Celebi, S. Gezici, K. Qaraqe, H. Arslan, and H. Poor, "Time-delay estimation in dispersed spectrum cognitive radio systems," *EURASIP Journal on Advances in Signal Processing*, vol. 23, Feb 2010.

[21] F. Wang, J. Huang, and Y. Zhao, "Delay sensitive communications over cognitive radio networks," *Wireless Communications, IEEE Transactions on*, vol. 11, no. 4, pp. 1402–1411, April 2012.

[22] F. P. Kelly, "Notes on effective bandwidths," in *Stochastic Networks: Theory and Applications*. Oxford University Press, 1996, no. 4, pp. 141–168.

[23] M. Hassan, M. Krunz, and I. Matta, "Markov-based channel characterization for tractable performance analysis in wireless packet networks," *IEEE Transactions on Wireless Communications*, vol. 3, no. 3, pp. 821–831, 2004.

[24] K. Park and W. Willinger, *Self-similar network traffic and performance evaluation*. Wiley Online Library, 2000.

[25] D. Anick, D. Mitra, and M. Sondhi, "Stochastic theory of a data handling system with multiple sources," in *Bell System Tech. Journal*, vol. 61, 1982, pp. 1871–1894.

[26] D. Mitra, "Stochastic theory of a fluid model of producers and consumers coupled by a buffer," in *Adv. Appl. Prob.*, vol. 20, 1988, pp. 646–676.

[27] Y. Liu and W. Gong, "On fluid queueing systems with strict priority," *IEEE Transactions on Automatic Control*, vol. 48, no. 12, pp. 2079–2088, 2003.

[28] B. Tan and S. Gershwin, "Modeling and analysis of markovian continuous flow systems with a finite buffer," *Annals of Operations Research*, vol. 182, no. 1, pp. 5–30, 2011.

[29] F. Roijers, H. V. D. Berg, and M. Mandjes, "Performance analysis of differentiated resource-sharing in a wireless ad-hoc network," *Performance Evaluation*, vol. 67, no. 7, pp. 528–547, 2010.

[30] N. Antunes, A. Pacheco, and R. Rocha, "An integrated traffic model for multimedia wireless networks," *Computer Networks*, vol. 38, no. 1, pp. 25–41, 2002.

[31] F. Wan, L. Cai, E. Shihab, and A. Gulliver, "Admission region of triple-play services in wireless home networks," *Computer Communications*, vol. 33, no. 7, pp. 852–859, 2010.

[32] V. Arunachalam, V. Gupta, and S. Dharmaraja, "A fluid queue modulated by two independent birth-death processes," *Computers & Mathematics with Applications*, vol. 60, no. 8, pp. 2433–2444, 2010.

[33] M. Krunz and J. G. Kim, "Fluid analysis of delay and packet discard performance for qos support in wireless networks," *Selected Areas in Communications, IEEE Journal on*, vol. 19, no. 2, pp. 384–395, Feb 2001.

[34] Q. Wang, D. Wu, and P. Fan, "Effective capacity of a correlated rayleigh fading channel," *Wireless Communications and Mobile Computing*, vol. 11, no. 11, pp. 1485–1494, 2011.

[35] M. Elalem and L. Zhao, "Effective capacity optimization for cognitive radio network based on underlay scheme in gamma fading channels," in *International Conference on Computing, Networking and Communications, ICNC*, 2013, pp. 714–718.

[36] D. Xu, Z. Feng, Y. Wang, and P. Zhang, "Capacity of cognitive radio under delay quality-of-service constraints with outdated channel feedback," 2012, pp. 1704–1709.

[37] S. Akin and M. Gursoy, "Effective capacity analysis of cognitive radio channels for quality of service provisioning," *IEEE Transactions on Wireless Communications*, vol. 9, no. 11, pp. 3354–3364, November 2010.

[38] P. Wang, D. Niyato, and H. Jiang, "Voice-service capacity analysis for cognitive radio networks," *IEEE Transactions on Vehicular Technology*, vol. 59, no. 4, pp. 1779–1790, 2010.

[39] L. Musavian and S. Aissa, "Effective capacity of delay-constrained cognitive radio in nakagami fading channels," *IEEE Transactions on Wireless Communications*, vol. 9, no. 3, pp. 1054–1062, March 2010.

[40] The President Council of Advisors on Science and Technology (PCAST). (2012, July) Report to the president: Realizing the full potential of government-held spectrum to spur economic growth. [Online]. Available: http://www.whitehouse.gov/sites/default/files/microsites/ostp/ pcast_spec trum_report_final_july_20_2012.pdf

[41] S. Asmussen, *Applied Probability and Queues*. New York: Springer-Verlag, 2003.

[42] C.-S. Chang, "Stability, queue length, and delay of deterministic and stochastic queueing networks," *IEEE Transactions on Automatic Control*, vol. 39, no. 5, pp. 913–931, 1994.

Prof. K.P. (Suba) Subbalakshmi is a Professor at Stevens Institute of Technology. Her research interests are in the areas of cognitive radio networks, wireless network security, media forensics as well as social networks. She is an Associate Editor of the IEEE Transactions on Vehicular Technology and IEEE Transactions on Cognitive Communications and Networking. She is the Founding Chair of the Security Special Interest Group of the IEEE Technical Committee on Cognitive Networks. She has given several keynote addresses, tutorials etc. at several international conferences. Suba is also the co-founder of two technology start-up companies, one on cognitive radio networks and the other based on deception detection on the Internet. She is a recipient of the Innovator award instituted by the NJ Inventor's Hall of Fame.

S. Ebrahim Safavi received the B.S. degree in Electrical Engineering from Isfahan Univ. of Tech., Iran in 2007 and his M.S. degree from Sharif Univ. of Tech, Iran in 2010. Since Fall 2010, he has been a Ph.D. student in the Department of Electrical and Computer Engineering, Stevens Institute of Technology, Hoboken, New Jersey, where he works in the iNFINITY lab. He was a recipient of Graduate Research Assistantship from Stevens Inst. of Technology. His research is mainly focused on wireless communication, cognitive radio networks and stochastic network characterization, in particular quality of service and performance evaluation. He is a student member of IEEE.

TABLE I: Notations

T_{f}	Channel free period random variable
T_{b}	Channel busy period random variable
λ_s	Active time exponential distribution parameter for SUs
μ_s	Idle time exponential distribution parameter for SUs
λ_p	Active / busy period exponential distribution parameter for PUs / channels
μ_p	Idle / free period exponential distribution parameter for PUs / channels
c_s	Traffic generation rate for each SU
c_p	Channel capacity for each PU
θ^*	Dominant decay rate for buffer over flow probability distribution
a^*	Effective bandwidth available to each SU
$P_{i,j}(\cdot)$	Cumulative distribution function of buffer occupancy

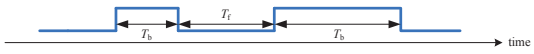

Fig. 1: Each channel is modeled as an ON-OFF process. The busy and free period random variables are denoted by T_{b} and T_{f}, respectively.

TABLE II: Simulation parameters

	Fig. 4	Fig. 5	Fig. 6a / 6b	Fig. 7a	Fig. 7b	Fig. 8
N_s	5	1	1	3	1	5
N_p	3	1	2	1	5	3
λ_s	2	-	-	1.2	-	1.2
μ_s	10	-	-	0.5	-	0.5
λ_p	6.7	0.6	0.4 / 0.8	-	0.7	0.7
μ_p	4.7	0.3	0.6 / 0.2	-	1	1
c_s	1	0.4	0.3 / 1.4	-	-	-
c_p	2.5	1	1	1.3	0.7	0.7
ϵ	-	10^{-3}	-	10^{-3}	10^{-3}	-

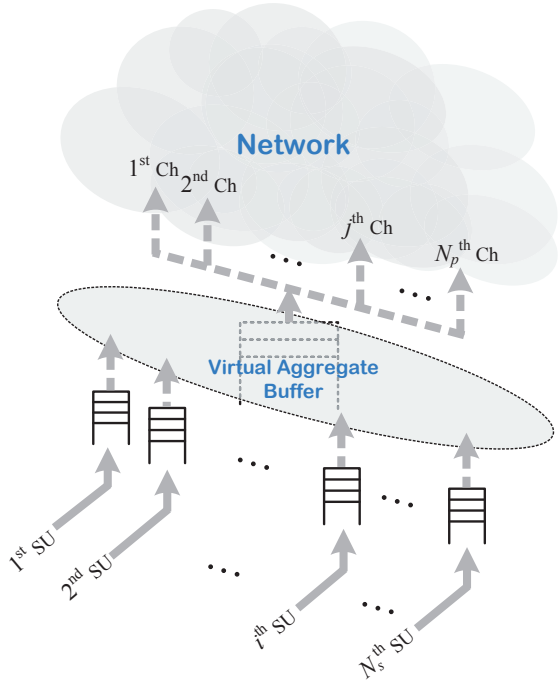

Fig. 2: Each channel is associated with a PU and is open for use by the SU only when the channel is unused by the corresponding PU. The data generated by the SU is placed in its own buffer. If a PU returns to the system, the SU can switch to the other available channels.

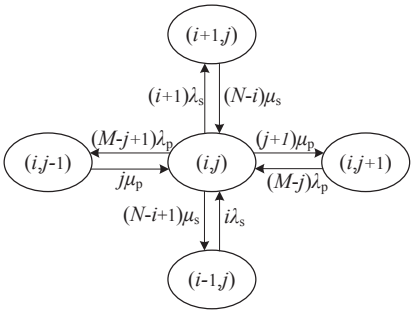

Fig. 3: The state transition diagram in steady state for the CTMC model.

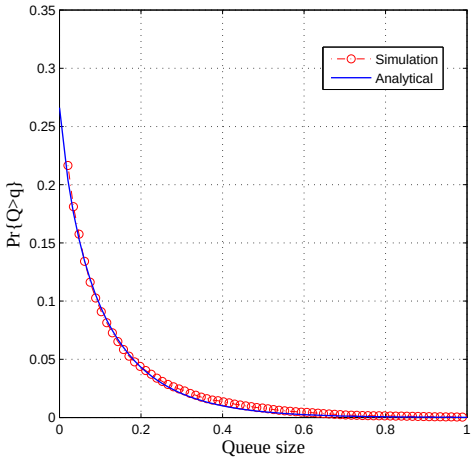

Fig. 4: A comparison of simulation and analytic results.

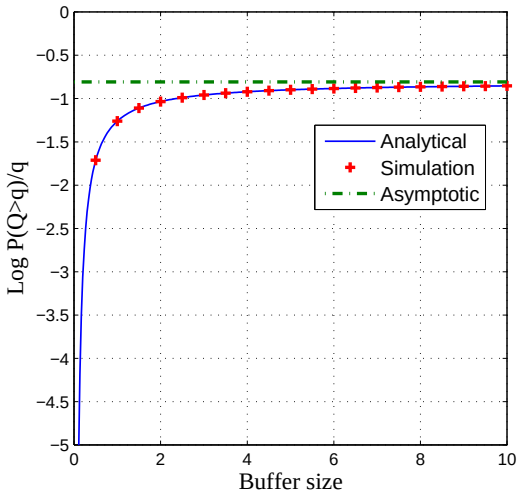

(a) Decay rate for buffer occupancy probability.

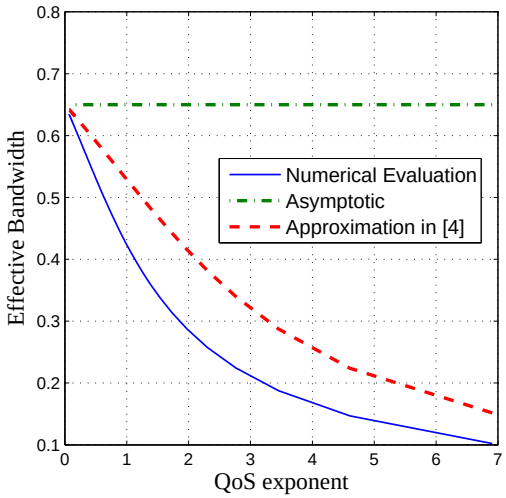

(b) Effective bandwidth versus QoS exponent parameter.

Fig. 5: The effective bandwidth of single SU, single PU network

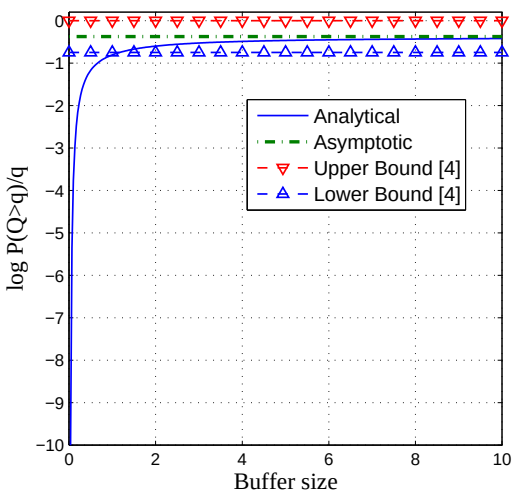

(a) $\log P(Q > q)/q$ vs Buffer size for $p_{11} = 0.4$ and $p_{01} = 0.6$

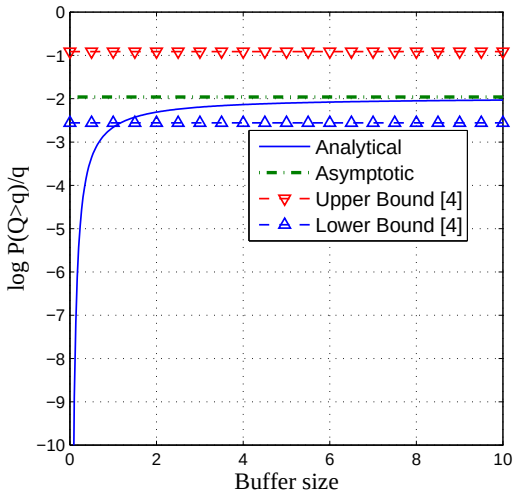

(b) $\log P(Q > q)/q$ vs Buffer size for $p_{11} = 0.8$ and $p_{01} = 0.2$

Fig. 6: The dominant decay rate for the network consisting of a single SU and two PUs.

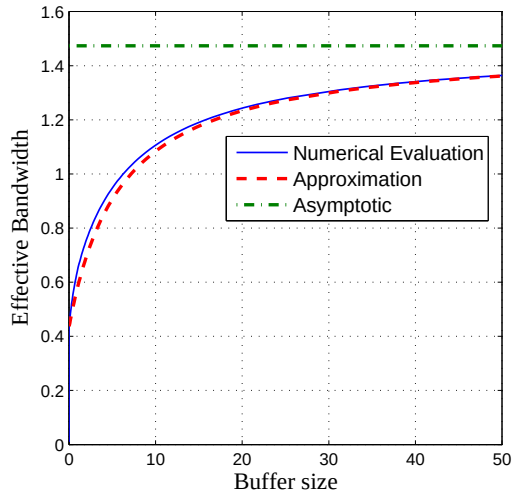

(a) Effective bandwidth for the system with single channel, multiple SUs. The approximation error is less than 1% for buffer size more than 10.

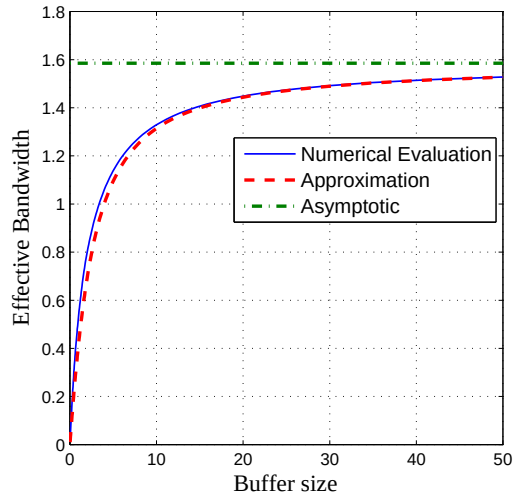

(b) Effective bandwidth for the system with single SU, multiple PUs. The approximation error is less than 2% for buffer size more than 10.

Fig. 7: The effective bandwidth vs. buffer size. Simulation shows that approximations derived in our study are very close to numerically evaluated analytical results.

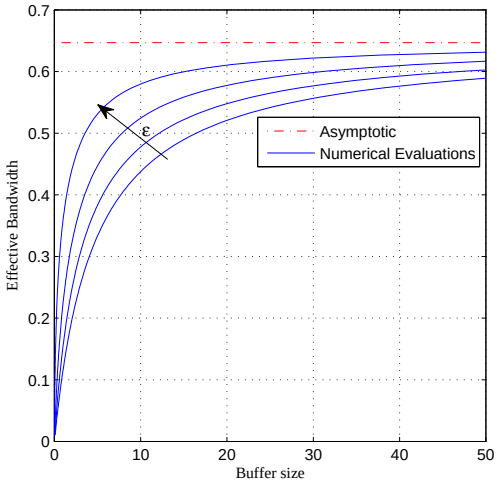

Fig. 8: Effective bandwidth for the system of multiple SUs, multiple channels for different ϵ QoS parameters